JOURNAL OF SOLID STATE CHEMISTRY **141,** 508–513 (1998)
ARTICLE NO. SC988006

Spectroscopic and Magnetic Properties of the MNi(AsO_4) (M = Li, Na) Arsenates and Crystal Structure Refinement of LiNi(AsO_4)

José L. Mesa,* José L. Pizarro,† Luis Lezama,* Jaione Escobal,* María I. Arriortua,† and Teófilo Rojo*,[1]

*Departamento de Química Inorgánica y †Departamento de Mineralogía-Petrología, Facultad de Ciencias, Universidad del País Vasco, Apdo. 644, E-48080 Bilbao, Spain

Received April 6, 1998; in revised form August 11, 1998; accepted August 12, 1998

Two compounds of general formula MNi(AsO_4) (M = Li, Na) have been synthesized and characterized by spectroscopic and magnetic techniques. The crystal structure of the LiNi(AsO_4) phase was refined using X-ray powder diffraction data. The compound crystallizes in the orthorhombic system, space group *Pnma*, $a = 10.284(2)$ Å, $b = 5.909(1)$ Å and $c = 4.853(1)$ Å. The lithium compound adopts the olivine structure, whereas the sodium phase exhibits a layered structure. Diffuse reflectance spectra for both compounds show bands belonging to Ni(II) ions in an octahedral environment. Magnetic susceptibility measurements indicate antiferromagnetic interactions for both the lithium and sodium compounds. The magnetic behavior of LiNi(AsO_4) is consistent with a 3D antiferromagnetic system, with an exchange parameter $J/k = -9.9$ K and a g-value of 2.19. The NaNi(AsO_4) phase exhibits 2D antiferromagnetic behavior, which was analyzed by using a honeycomb model. The J/k value obtained is -7.0 K, with $g = 2.20$. © 1998 Academic Press

INTRODUCTION

$M^{I}M^{II}(XO_4)$ (M^{I} = Li, Na, etc., M^{II} = Co, Ni, Mg, etc., and X = P, As) are members of a family of compounds of the $ABXO_4$ type in which A and B are mono- and divalent cations, respectively. Different structure types are adopted by the phosphates of this stoichiometry depending on the relative sizes of the A and B ions. When the A and B ions have similar radii, as in the case of compounds in which B is an alkaline earth metal, such as Ca^{2+}, Sr^{2+}, or Ba^{2+}, and A is Na^{+}, K^{+}, or Rb^{+}, the arcanite (β-K_2SO_4) structure type is adopted (1–4). When the size of the B cation is small, as in the case of Mg^{2+} and some transition metal ions, such as Mn^{2+}, Fe^{2+}, Ni^{2+}, Co^{2+}, or Zn^{2+}, two different families have been observed depending on the size of the A cations. If the A ions are relatively large ($A = K^{+}$, Rb^{+}, Cs^{+}, NH_4^{+}, etc.), the phosphates have the trydimite-type structure (β-deformation of SiO_2) (5–8). However, for A cations of small size, as in the case of Li^{+}, the resulting compounds, $LiM(PO_4)$ (M = Mn, Fe, Co, Ni, Mg, etc.), adopt the olivine (Mg_2SiO_4) type structure (9). The structures of arsenate compounds with $M^{I}M^{II}(AsO_4)$ stoichiometry have been less studied in comparison with those of the phosphate compounds.

The crystal structure of LiNi(AsO_4) has not been reported. However, it is known that isostructural LiNi(PO_4) adopts the olivine structure (10). The crystal structure of the olivine type consists of a hexagonal close packing of oxygen with Li and Ni located in half of the octahedral sites and P in one eighth of the tetrahedral sites. The NiO_6 distorted octahedra are corner shared and cross-linked by the PO_4 groups, forming a three-dimensional network, with perpendicular tunnels along the [010] and [001] directions, in which the Li^{+} ions are inserted (Fig. 1) (11).

NaNi(AsO_4) has a pronounced layer structure, as for the related KNi(AsO_4) phase (12). The structure of NaNi(AsO_4) is built up from tetrahedral–octahedral–tetrahedral three-layer units. These three-layer units are stacked along the [001] direction, giving a layer spacing $c/3 = 8.82$ Å. Each of the three-layer units is built up from a central two-dimensional infinite octahedral layer of composition Ni_2O_3, which is enclosed by two AsO_4 tetrahedral layers. The sodium atoms are placed in the tetrahedral layers and occupy isolated tetrahedra, the coordination for these ions being (4 + 3) (Fig. 2a) (13). The structure can also be described as parallel honeycomb-like sheets, each consisting of an infinite hexagonal array of NiO_6 octahedra (Fig. 2b).

In this work we present the spectroscopic and magnetic properties of two nickel arsenate compounds belonging to the $M^{I}M^{II}(XO_4)$ family. One of them, the lithium phase, exhibits 3D antiferromagnetic interactions and the other one, the sodium compound, shows 2D antiferromagnetic behavior. The crystal structure of LiNi(AsO_4) has been refined by using X-ray diffraction powder data.

[1]To whom correspondence should be addressed. E-mail: qiproapt@lg.ehu.es.

0022-4596/98 $25.00
Copyright © 1998 by Academic Press
All rights of reproduction in any form reserved.

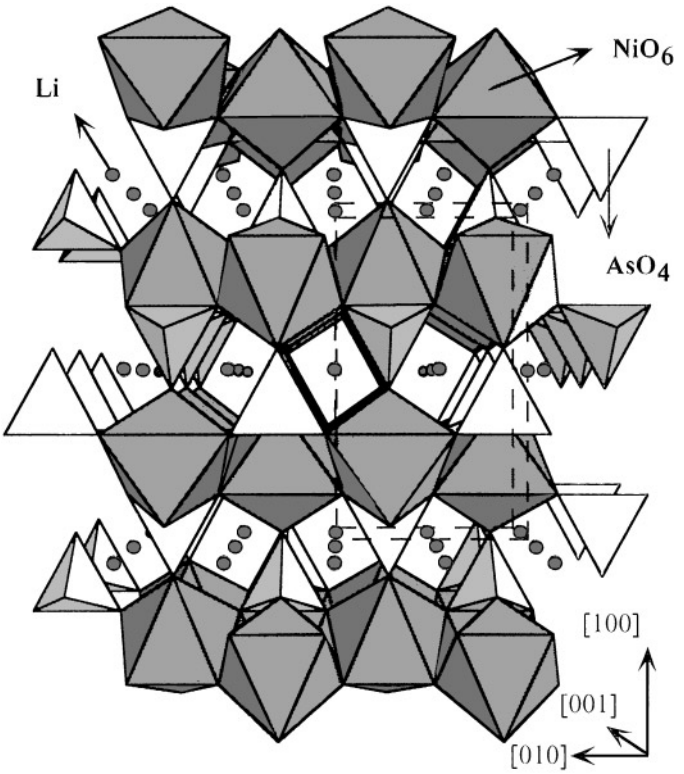

FIG. 1. Crystal structure of LiNi(AsO$_4$).

EXPERIMENTAL

Preparation of the Compounds

The MNi(AsO$_4$) (M = Li, Na) compounds were prepared by solid-state reactions in air starting from LiOH·H$_2$O, Ni(NO$_3$)$_2$·6H$_2$O, and NH$_4$H$_2$AsO$_4$ for the LiNi(AsO$_4$) phase and using the NaHCO$_3$, Ni(NO$_3$)$_2$·6H$_2$O, and NH$_4$H$_2$AsO$_4$ salts for the preparation of NaNi(AsO$_4$). Stoichiometric quantities of these materials were ground together in an agate mortar. The resulting mixtures were heated in an open crucible at 600°C to decompose all initial reactants. This process was followed by further heating at 800°C for 20 h with an intermediate regrinding after 10 h. The final products were quenched to room temperature.

Lithium, sodium, nickel, and arsenic contents were determined by ICP-AES analysis. The results were consistent with the following stoichiometries: LiNi(AsO$_4$) (Found: Li, 3.3; Ni, 28.5; As, 36.3. Calc: Li, 3.4; Ni, 28.7; As, 36.6%); NaNi(AsO$_4$) (Found: Na, 10.3; Ni, 26.4; As, 33.7. Calc: Na, 10.4; Ni, 26.6; As, 34.0%).

X-Ray Crystallography

The X-ray powder diffraction pattern of LiNi(AsO$_4$), used for the Rietveld analysis, was collected with a STOE (Darmstadt) automatic diffractometer. Monochromated

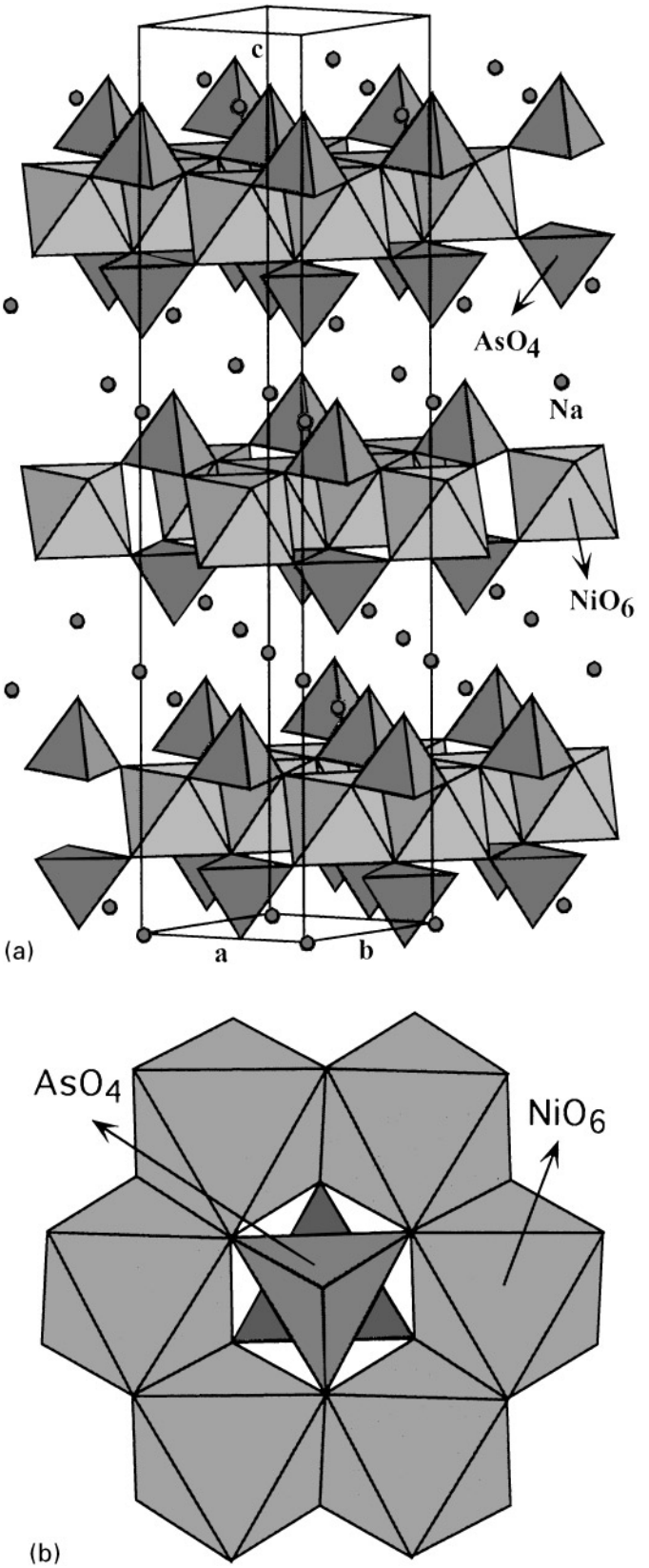

FIG. 2. (a) Crystal structure of NaNi(AsO$_4$). (b) View of the structure showing the packing of the NiO$_6$ octahedra.

Cu$K\alpha_1$ radiation was employed. An ω–2θ scan was performed, with steps of 0.02° in 2θ and a fixed-time counting of 12 s. Rietveld full-profile refinement was performed with the FULLPROF program (14), starting from the structural parameters of $LiNi(PO_4)$ (10). $Li_3(AsO_4)$ (15) was detected as an impurity phase in the X-ray powder diffraction pattern of $LiNi(AsO_4)$ and was included in the Rietveld refinement. Details of the process are given in Table 1. The observed, calculated, and difference X-ray powder diffraction patterns are shown in Fig. 3.

The pattern of $NaNi(AsO_4)$, recorded with steps of 0.05° in 2θ and a fixed-time counting of 6 s, was indexed by using the LSUCRE program (16) in a rhombohedral unit cell with the $R\bar{3}$ space group, as previously determined from X-ray single-crystal data by Jones (17). The refined parameters are $a = 4.944(6)$ Å, $c = 26.446(5)$ Å, and $D_{calc} = 3.941\ g \cdot cm^{-3}$. The parameters given in the literature are $a = 4.955(3)$ Å, $c = 26.47(3)$ Å, and $D_{calc} = 3.905\ g \cdot cm^{-3}$ (17).

Physical Measurements

IR spectra (KBr pellets) were obtained with a Nicolet FT-IR 740 spectrophotometer. Diffuse reflectance spectra were registered at room temperature on a Cary 2415 spectrometer in the range 5,000–45,000 cm^{-1}. Magnetic measurements were performed on polycrystalline samples between 1.8 and 300 K, using a Quantum Design SQUID magnetometer (MPMS-7) with a magnetic field of 0.1 T at which the magnetization vs magnetic field is linear even at 1.8 K.

TABLE 1
Summary of Crystallographic Data and Least-Squares Refinement for $LiNi(AsO_4)$

Compound	$LiNi(AsO_4)$
M_r ($g \cdot mol^{-1}$)	204.6
Crystal system	Orthorhombic
Space group (No. 53)	*Pnma*
a (Å)	10.284(2)
b (Å)	5.909(1)
c (Å)	4.853(1)
V (Å^3)	294.9(1)
T (K)	298
Radiation	Cu$K\alpha_1$
Monochromator	Ge
Z	4
D_{calc} ($g \cdot cm^{-3}$)	2.77
2θ range (deg)	5–110
2θ step–scan increment (deg)	0.02
Time–step (s/step)	12
Number of reflections	207
Number of structural parameters	18
Number of profile parameters	15
$R_p = \Sigma\lvert y_{i,obs} - (1/c) y_{i,calc}\rvert / \Sigma y_{i,obs}$	15.0
$R_{wp} = [\Sigma wi\lvert y_{i,obs} - (1/c) y_{i,calc}\rvert^2 / \Sigma wi[y_{i,obs}]^2]^{1/2}$	16.4
$R_B = \Sigma\lvert I_{obs} - I_{calc}\rvert / \Sigma I_{obs}$	10.3
GOF	3.60

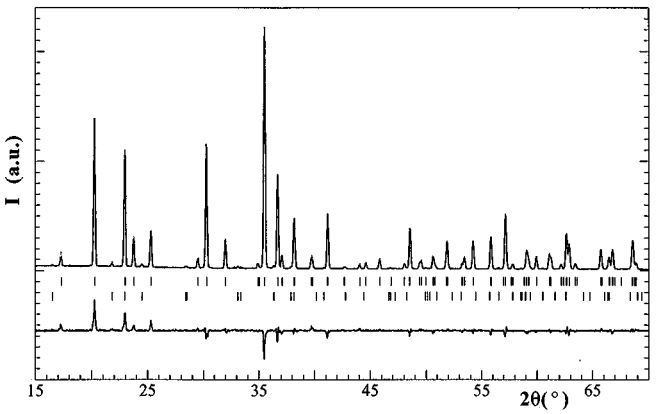

FIG. 3. Observed, calculated, and difference X-ray powder diffraction patterns of $LiNi(AsO_4)$. The observed data are shown by the dots; the calculated pattern is shown by the solid line.

RESULTS AND DISCUSSION

Structural Study

Atomic coordinates for $LiNi(AsO_4)$ are given in Table 2. Interatomic bond distances and angles are presented in Table 3.

$LiNi(AsO_4)$ adopts an olivine-type structure in which the Li^+ cations are hexacoordinated, with Li–O(1)^{i} = 2.133(4) Å, Li–O(2)^{ii} = 2.201(4) Å, and Li–O(3) = 2.214(5) Å. The mean value of the cis angles O_{cis}–Li–O_{cis}, which range from 71.3(2)° to 108.7(2)°, is 90(12)° whereas the mean value of the trans basal angles O_{trans}–Li–O_{trans} is 180°. The Ni^{2+} cations are also hexacoordinated and give rise to more distorted octahedra. The coordination polyhedron is formed by two oxygen atoms O(3)^{iii} with bond distances of 2.180(5) Å and four shorter bond distances Ni–O(1), Ni–O(2)^{iii}, and Ni–O(3)^{iv} of 2.071(7), 2.026(7), and 2 × 2.078(5) Å, respectively. The mean value of the cis angles O_{cis}–Ni–O_{cis}, which range from 69.8(2)° to 110.4(2)°, is 90(12)°. For the trans basal angles O_{trans}–Ni–O_{trans}, which range from 159.3(2)° to 175.1(2)°, the mean value is 164(8)°.

TABLE 2
Fractional Atomic Coordinates and Equivalent Isotropic Displacement Parameters (Å^2) for $LiNi(AsO_4)$

Atom	Site	x	y	z	B_{eq}[a]
Li	4*a*	0	0	0	4.1(4)
Ni	4*c*	0.2728(1)	1/4	0.9927(3)	4.0(5)
As	4*c*	0.0953(1)	1/4	0.4343(2)	3.6(3)
O(1)	4*c*	0.1017(7)	1/4	0.768(1)	3.2(1)
O(2)	4*c*	0.4484(7)	1/4	0.182(1)	3.4(2)
O(3)	8*d*	0.1668(6)	0.0389(7)	0.2846(9)	3.5(1)

[a] $B_{eq} = (8\pi^2/3)\ \Sigma_i\Sigma_j U_{ij} a_i a_j \mathbf{a}_i \cdot \mathbf{a}_j$.

TABLE 3
Bond Distances (Å) and Angles (Deg) for LiNi(AsO$_4$)[a]

Bond distances

LiO_6 octahedron		NiO_6 octahedron	
Li–O(1)^{i}	2.133(4) × 2	Ni–O(1)	2.071(7)
Li–O(2)^{ii}	2.201(4) × 2	Ni–O(2)^{iii}	2.026(7)
Li–O(3)	2.214(5) × 2	Ni–O(3)^{iv}	2.078(5) × 2
		Ni–O(3)^{iii}	2.180(5) × 2
AsO_4 tetrahedron			
As–O(1)	1.619(6)		
As–O(2)^{v}	1.613(7)		
As–O(3)^{vi}	1.620(5) × 2		

Bond angles

LiO_6 octahedron		NiO_6 octahedron	
O(3)–Li–O(1)^{i}	83.0(2) × 2	O(2)^{iii}–Ni–O(3)^{iii}	98.7(2) × 2
O(3)–Li–O(1)^{vii}	97.0(2) × 2	O(2)^{iii}–Ni–O(3)^{ix}	87.4(2) × 2
O(3)–Li–O(2)^{ii}	108.7(2) × 2	O(1)–Ni–O(3)^{x}	85.3(2) × 2
O(3)–Li–O(2)^{v}	71.3(2) × 2	O(1)–Ni–O(3)^{iv}	89.9(2) × 2
O(1)^{i}–Li–O(2)^{ii}	88.6(1) × 2	O(3)^{iii}–Ni–O(3)^{ix}	89.7(2) × 2
O(1)^{i}–Li–O(2)^{v}	91.4(1) × 2	O(3)^{iii}–Ni–O(3)^{x}	69.8(2)
O(3)–Li–O(3)^{viii}	180.0(4)	O(3)^{ix}–Ni–O(3)^{iv}	110.4(2)
O(2)^{ii}–Li–O(2)^{v}	180.0(4)	O(1)–Ni–O(2)^{iii}	175.1(2)
O(1)^{i}–Li–O(1)^{vii}	180.0(3)	O(3)^{iii}–Ni–O(3)^{iv}	159.3(2)
		O(3)^{ix}–Ni–O(3)^{x}	159.3(2)
AsO_4 tetrahedron			
O(1)–As–O(2)^{v}	112.8(3)		
O(1)–As–O(3)^{vi}	115.4(2) × 2		
O(2)^{v}–As–O(3)^{vi}	105.6(2) × 2		
O(3)–As–O(3)^{vi}	100.7(2)		

[a] Symmetry codes: i = $x, y, z-1$, ii = $-x+1/2, -y, z-1/2$, iii = $x, y, z+1$, iv = $-x+1/2, y+1/2, z+1/2$, v = $x-1/2, y, 1/2-z$, vi = $x, -y+1/2, z$, vii = $-x, -y, -z+1$, viii = $-x, -y, -z$, ix = $-x+1/2, -y, z+1/2$, x = $x, -y+1/2, z+1$.

The arsenate group exhibits three different bond lengths and four different bond angles, with mean values of 1.617(7) Å and 108(6)°, respectively.

Spectroscopic Study

The IR spectra of the title compounds show three important groups of bands. The bands observed in the 900 to 600-cm^{-1} region are attributed to the stretching vibration modes of the $(AsO_4)^{3-}$ groups. The ν_3 asymmetrical stretching mode [ν_{as}(As–O)] appears at 900, 845, and 785 cm^{-1} for LiNi(AsO$_4$). The ν_1 symmetrical stretch [ν_s(As–O)] is detected at 640 cm^{-1}. The asymmetrical deformation vibrations [δ_{as}(O–As–O)] can be observed at 540 and 430 cm^{-1}. The frequencies at which these bands appear are lower than those observed in the analogous phosphate, LiNi(PO$_4$), which are 1140, 1080, and 965 cm^{-1} for ν_3, at 660 cm^{-1} for ν_1, and 580, 545, and 465 cm^{-1} for the deformation modes (18). The variation is in accordance with longer bond lengths in the arsenate groups. For NaNi(AsO$_4$) the ν_3 asymmetrical stretching mode is observed at 925, 865, and 770 cm^{-1}. The ν_1 symmetrical stretch appears at 590 cm^{-1}. The asymmetrical deformation vibrations are detected at 465 and 420 cm^{-1}. The positions of these bands are similar to those observed in the LiNi(AsO$_4$) phase, in good agreement with the presence of arsenate groups, with similar bond distances (13, 17). Finally, the bands in the lower frequency region of the spectra, which appear at 365 and 320 cm^{-1} for LiNi(AsO$_4$) and at 370 and 330 cm^{-1} for NaNi(AsO$_4$), can be attributed to the stretching vibrations of the metal–oxygen bonds according to that observed in other related arsenates (19–22).

The diffuse reflectance spectra of the MNi(AsO$_4$) (M = Li, Na) compounds exhibit the same essential features. Three broad absorption bands ascribed to the spin-allowed transitions $^3A_{2g} \rightarrow {}^3T_{2g}$, $^3T_{1g}(F)$, and $^3T_{1g}(P)$ were observed at the following frequencies: $\nu_1 = 7875$, $\nu_2 = 12{,}500$, and $\nu_3 = 23{,}530$ cm^{-1} for LiNi(AsO$_4$) and $\nu_1 = 7850$, $\nu_2 = 13{,}160$, and $\nu_3 = 23{,}530$ cm^{-1} for NaNi(AsO$_4$). The spin-forbidden transitions $^3A_{2g} \rightarrow {}^1E_g$, and $^1T_{2g}$ were also observed at $\nu_4 = 14{,}085$ and $\nu_5 = 21{,}275$ cm^{-1} for the lithium arsenate and $\nu_4 = 13{,}890$ and $\nu_5 = 21{,}055$ cm^{-1} for the sodium arsenate. The Dq and Racah parameters, calculated by fitting the experimental frequencies to an energy-level diagram for octahedral d^8 systems (23), are $Dq = 790$, $B = 965$, and $C = 3535$ cm^{-1} for the lithium compound and $Dq = 785$, $B = 945$, and $C = 3505$ cm^{-1} for the sodium compound. These values are in the range usually found for octahedrally coordinated Ni(II) compounds (21–23).

Magnetic Study

The temperature dependences of both the magnetic molar susceptibility, χ_m, and the product $\chi_m T$ for LiNi(AsO$_4$) are shown in Fig. 4. The thermal evolution of χ_m satisfies the Curie–Weiss law at high temperatures, with $C_m = 1.26$ cm^3 K mol^{-1} and $\theta = -104.2$ K, exhibiting a maximum in χ_m centered at 55 K. This result together with the continuous decrease in the $\chi_m T$ values is indicative of antiferromagnetic exchange couplings in the compound. At lower temperatures, a small increase is observed that can be attributed to the presence of a small amount of a paramagnetic impurity in the sample (< 3%), which was not detected by X-ray powder diffraction data.

Owing to the structural findings for LiNi(AsO$_4$), the simple cubic 3D Heisenberg antiferromagnetic model for $S = 1$ can be considered for the analysis of the magnetic behavior. In this way, it was possible to fit the χ_m experimental values using the expression of Rushbrook and Wood (24):

$$\chi = (2Ng^2\beta^2/3kT)(1 + Ax + Bx^2 + Cx^3 + Dx^4 + Ex^5 + Fx^6)^{-1}, \quad [1]$$

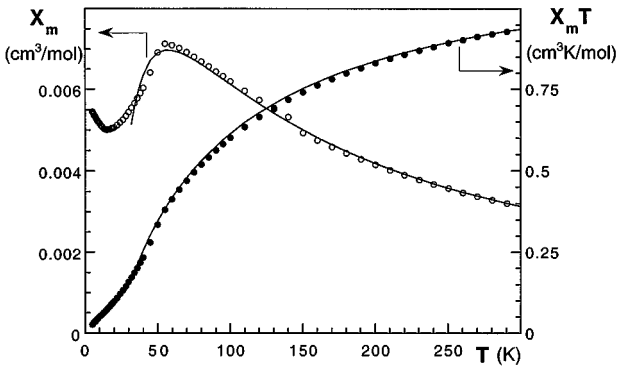

FIG. 4. Temperature dependence of χ_m and $\chi_m T$ for $LiNi(AsO_4)$. The circles are the experimental values and the full lines represent the theoretical values for a 3D Heisenberg model.

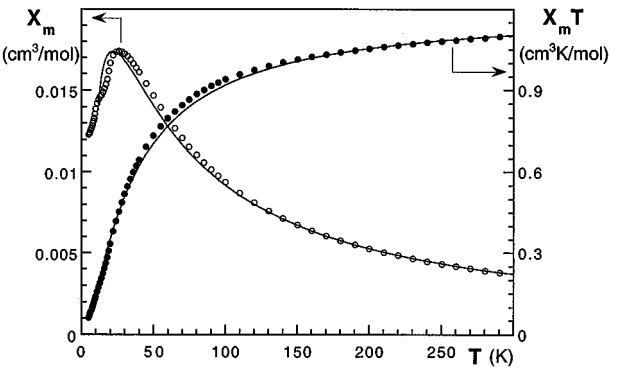

FIG. 5. Temperature dependence of χ_m and $\chi_m T$ for $NaNi(AsO_4)$. The circles are the experimental values and the full lines represent the theoretical values for a 2D honeycomb model.

where $x = |J|/kT$, $k = 1.3807 \times 10^{-16}$ erg K^{-1}, N is Avogadro's number, $\beta = 9.274 \times 10^{-21}$ erg G^{-1}, $A = 8$, $B = 14.66667$, $C = 14.2222$, $D = 61.185$, $E = 162.449$, and $F = 1127.96$. Equation [1] is valid only up to a certain temperature, since it becomes not quantitative when the ratio kT/J approaches unity, because only a small number of terms (six) are known in the infinite series. As can be seen in Fig. 4, this result shows good agreement between the experimental data and the three-dimensional Heisenberg model. The best fit of the experimental data to the above equation was obtained for $J/k = -9.9$ K and $g = 2.19$, which is a usual value for octahedral Ni(II) ions.

Considering the structural features in the $LiNi(AsO_4)$ phase, at least three different magnetic exchange pathways could be deduced. One of them involves the $d_{x^2-y^2}$ orbital from the corner-shared NiO_6 octahedra, leading to an antiferromagnetic coupling inside the (011) crystallographic plane. A second pathway could be considered inside this (011) plane through the AsO_4 groups, which leads to weaker ferromagnetic interactions. The third exchange pathway implies the interactions through the d_z^2 orbital of the Ni(II) ions along the [100] direction, involving the AsO_4 groups. These interactions are preferentially antiferromagnetic, as was observed for other transition metal phosphates (25). Thus, the full magnetic system can be described as a three-dimensional antiferromagnetic net.

For $NaNi(AsO_4)$ the temperature dependences of both the magnetic susceptibility and $\chi_m T$ are shown in Fig. 5. The thermal evolution of χ_m satisfies the Curie–Weiss law at high temperatures with $C_m = 1.20$ cm^3 K mol^{-1} and $\theta = -28.3$ K and exhibits a maximum centered at 30 K. This result and the continuous decrease in $\chi_m T$ are indicative of antiferromagnetic interactions in the compound.

The 2D planar honeycomb model for the $S = 1$ antiferromagnetic system, considering only magnetic interactions between the nickel(II) ions arranged inside the layers, was used for the analysis of the magnetic behavior. The χ_m experimental values were fitted using the expression of Rushbrook and Wood (24), Eq. [1], where $A = 4$, $B = 7.333$, $C = 7.111$, $D = -5.703$, $E = -22.281$, and $F = 51.737$. From Fig. 5 one can observe a reasonable agreement between the experimental data and the theoretical model. The value obtained for the magnetic exchange parameter is $J/k = -7.0$ K, with $g = 2.20$. Attempts to evaluate the possible interlayer interactions by means of a J' parameter treated in the molecular field approximation (26) lead to extremely low values without a significant improvement of the fit.

Considering the structural features in the $NaNi(AsO_4)$ phase, we see that the main magnetic exchange pathway involves the $d_{x^2-y^2}$ orbitals from the NiO_6 edge-shared octahedra, leading to an antiferromagnetic coupling within the layers.

CONCLUDING REMARKS

The $MNi(AsO_4)$ (M = Li, Na) compounds exhibit different crystal structures. The lithium phase adopts an olivine-type structure, whereas the sodium compound shows a layered structure which consists of an infinite hexagonal array of NiO_6 octahedra enclosed by two AsO_4 tetrahedral layers. The transitions observed in the diffuse reflectance spectra of the compounds are indicative of Ni(II) ions in approximately octahedral symmetry with Dq and Racah parameters usually found for this ion. Magnetic measurements are consistent with the existence of antiferromagnetic interactions in the compounds. The $LiNi(AsO_4)$ phase exhibits a 3D magnetic behavior, whereas $NaNi(AsO_4)$ is a 2D magnetic system, with a honeycomb-like layer structure.

ACKNOWLEDGMENTS

This work was financially supported by the Government of the Basque Country (grant PGV PI97/106), which we gratefully acknowledge. J.E. thanks the UPV/EHU for a doctoral fellowship.

REFERENCES

1. M. Ben Amara, M. Vlasse, G. Le Flem, and P. Hagenmuller, *Acta Crystallogr*, *Sect*. *C* **39,** 1483 (1983).
2. R. Klement and P. Kresse, *Z*. *Anorg. Allg. Chem.* **310,** 53 (1961).
3. A. W. Kolsi, M. Quarton, and W. Freundlich, *J*. *Solid State Chem.* **36,** 107 (1981).
4. C. W. Struck, and J. G. White, *Acta Crystallogr*. **15,** 290 (1962).
5. O. V. Yakubovich, M. A. Simonov, and O. K. Melnikov, *Kristallografiya* **35,** 42 (1990).
6. M. Lujan, F. Kubel, and H. Schmid, *Z*. *Naturforsch*, *B* **49,** 1256 (1994).
7. M. Andratschke, K. J. Range, H. Haase, and U. Klement, *Z*. *Naturforsch B* **47,** 1249 (1992).
8. L. Elammari and B. Elouadi, *J*. *Chim. Phys.* **88,** 1969 (1991).
9. H. D. Megaw, *in* "Crystal Structures: A Working Approach," p. 249. Saunders, London, 1973.
10. I. Abrahams and K. S. Easson, *Acta Crystallogr Sect. C* **49,** 925 (1993).
11. S. Geller and J. L. Durand, *Acta Crystallogr*. **13,** 325 (1960).
12. A. M. Buckley, S. T. Bramwell, and P. Day, *Z*. *Naturforsch.* **44,** 1053 (1988).
13. K. J. Range and H. Meister, *Z*. *Naturforsch. B* **39,** 118 (1984).
14. J. Rodriguez-Carvajal, FULLPROF, "Program Rietveld Pattern Matching Analysis of Powder Patterns," ILL, Grenoble, 1994 (unpublished).
15. A. Elfakir, G. Wallez, M. Quarton, and J. Pannetier, *Phase Transitions* **45,** 281 (1993).
16. D. E. Appleman and K. T. Evans, "*Indexing and Least-Squares Refinement of Powder Diffraction Data*," NTIS Document PB-216188, 1973.
17. P. G. Jones, *Z*. *Naturforsch B* **42,** 1365 (1987).
18. A. Goñi, Ph.D. Thesis, University of Basque Country, 1997.
19. R. J. Hill, *Am. Mineral.* **61,** 979 (1976).
20. R. S. W. Braithwaite, *Mineral*. *Mag*. **47,** 51 (1983).
21. J. M. Rojo, J. L. Mesa, J. L. Pizarro, L. Lezama, M. I. Arriortua, and T. Rojo, *Mater*. *Res. Bull*. **31,** 925 (1996).
22. J. M. Rojo, J. L. Mesa, J. L. Pizarro, L. Lezama, M. I. Arriortua, and T. Rojo, *J*. *Solid State Chem.* **132,** 107 (1997).
23. A. B. P. Lever, "Inorganic Electronic Spectroscopy." Elsevier, Amsterdam/New York, 1984.
24. G. S. Rushbrook and P. J. Wood, *Mol*. *Phys.* **1,** 257 (1958).
25. L. Lezama, K. S. Suh, G. Villeneuve, and T. Rojo, *Solid State Commun.* **76,** 449 (1990).
26. M. E. Fisher, *Am*. *J*. *Phys.* **32,** 343 (1964).